The SM protein Sly1 accelerates assembly of the ER–Golgi SNARE complex

F. Esra Demircioglu[a,1], Pawel Burkhardt[a,2], and Dirk Fasshauer[a,b,3]

[a]Research Group Structural Biochemistry, Department of Neurobiology, Max Planck Institute for Biophysical Chemistry, 37077 Göttingen, Germany; and [b]Department of Fundamental Neurosciences, University of Lausanne, 1005 Lausanne, Switzerland

Edited by Peter J. Novick, University of California, San Diego, La Jolla, CA, and approved August 14, 2014 (received for review May 5, 2014)

Soluble *N*-ethylmaleimide–sensitive factor attachment protein receptor (SNARE) and Sec1/Munc18 (SM) proteins constitute the core of an ancient vesicle fusion machine that diversified into distinct sets that now function in different trafficking steps in eukaryotic cells. Deciphering their precise mode of action has proved challenging. SM proteins are thought to act primarily through one type of SNARE protein, the syntaxins. Despite high structural similarity, however, contrasting binding modes have been found for different SM proteins and syntaxins. Whereas the secretory SM protein Munc18 binds to the "closed conformation" of syntaxin 1, the ER–Golgi SM protein Sly1 interacts only with the *N*-peptide of Sed5. Recent findings, however, indicate that SM proteins might interact simultaneously with both syntaxin regions. In search for a common mechanism, we now reinvestigated the Sly1/Sed5 interaction. We found that individual Sed5 adopts a tight closed conformation. Sly1 binds to both the closed conformation and the *N*-peptide of Sed5, suggesting that this is the original binding mode of SM proteins and syntaxins. In contrast to Munc18, however, Sly1 facilitates SNARE complex formation by loosening the closed conformation of Sed5.

membrane fusion | ER–Golgi trafficking | protein–protein interaction | isothermal titration calorimetry | fluorescence spectroscopy

In eukaryotic cells, material is transported in vesicles that pinch off of one set of membranes and move along microtubule tracks to the next compartment, where they specifically fuse. Key players in the fusion of a vesicle with its acceptor membrane are the soluble N-ethylmaleimide–sensitive factor attachment protein receptor (SNARE) proteins. Heterologous sets of SNARE proteins drive the fusion of two membranes by zippering into a tight four-helix bundle structure. Distinct sets of SNARE proteins carry out different vesicle fusion steps in the cell. An essential SNARE protein for transport into and across the Golgi is Sed5/syntaxin 5 (1). Besides SNARE complexes, Sed5 exists also in a 1:1 complex with the Sec1/Munc18 (SM) protein Sly1 that is essential for ER–Golgi and intra-Golgi trafficking (2). Distinct types of SM proteins are thought to function together with the respective SNARE complex, specifically its syntaxin (reviewed in refs. 3–8).

The very N-terminal region, the so-called *N*-peptide, of Sed5 binds with nanomolar affinity to the outer surface of Sly1 (9–12). This mode of interaction is consistent with the notion that Sly1 can stay bound during SNARE complex formation and that it might even be actively involved in this reaction (13). This idea was strengthened by the observation that Sec1, the SM protein essential for secretion in yeast, interacts with the assembled SNARE complex but not with its isolated syntaxin (14). Unfortunately, for the interaction of Sec1 with its SNARE unit, no definitive structural foundation exists so far, and it remains uncertain whether Sec1 can be considered as a model for SM protein function. Fortunately, the animal counterpart of Sec1, Munc18-1, has been studied in more detail. However, the results of numerous biochemical studies on Munc18-1 appear not to fit into the concept of SM proteins being factors that promote SNARE assembly. On the contrary, initial studies found that Munc18-1 strongly interferes with the ability of its cognate syntaxin 1 to form a SNARE complex (15, 16). This inhibition is difficult to reconcile with an essential role of Munc18-1 during neurotransmitter release (17). The structure of the Munc18-1/syntaxin 1a complex revealed that the central cavity of Munc18-1 wraps around syntaxin in the so-called "closed conformation" (18). In this conformation, the three-helix bundle formed by syntaxin's N-terminal Habc domain folds back onto its SNARE motif (19), restricting the availability of syntaxin for its SNARE partners. Thus, although they share a similar structure, Munc18-1 and Sly1 appear to bind to their cognate syntaxins in different modes.

New light on this discrepancy was shed when it was discovered that Munc18-1 is able to bind simultaneously to a second, spatially separated binding site on syntaxin 1 (15). This second site involves the *N*-peptide region of syntaxin 1 that, similar to the Sed5 *N*-peptide (12), binds to the outer surface of Munc18-1. Interestingly, both binding sites are also present in the Munc18/syntaxin 1 complex of the choanoflagellate *Monosiga brevicollis* (20). This suggests that the binding mode involving two different sites is evolutionarily conserved. A comparable binding mode was also described for the SM protein Vps45, which regulates trans-Golgi network trafficking. Vps45 binds tightly to the *N*-peptide of its cognate syntaxin Tlg2/syntaxin 16 (21). It was shown later that Vps45 is also able to interact with the remainder of its Qa-SNARE, possibly in a closed conformation (15, 22).

Not all SM proteins are known to bind to the *N*-peptide of their cognate syntaxin. For example, in the SM protein Vps33, which plays an essential role in the degradation pathway, the *N*-peptide binding pocket is blocked (23, 24). Vps33 is part of

Significance

Every vesicle fusion reaction is driven by soluble N-ethylmaleimide–sensitive factor attachment protein receptor (SNARE) proteins that zipper into tight complexes between membranes. Members of the Sec1/Munc18 (SM) family tightly regulate this process through interactions with a member of the syntaxin SNARE subfamily. However, seemingly different interaction modes have been found for different SM proteins and syntaxins. Here we show that the ER–Golgi SM protein Sly1 interacts not only with the N-peptide of the syntaxin Sed5, as previously thought, but also with its remainder. This corroborates the idea that SM proteins and syntaxins generally make use of two spatially separated binding sites. Remarkably, binding of Sly1 relaxes the autoinhibitory closed conformation of Sed5 and thereby accelerates SNARE complex formation.

Author contributions: F.E.D. and D.F. designed research; F.E.D. and P.B. performed research; F.E.D., P.B., and D.F. analyzed data; and F.E.D. and D.F. wrote the paper.

The authors declare no conflict of interest.

This article is a PNAS Direct Submission.

[1]Present address: Department of Biology, Massachusetts Institute of Technology, Cambridge, MA 02139.

[2]Present address: Department of Molecular and Cell Biology, University of California, Berkeley, CA 94720.

[3]To whom correspondence should be addressed. Email: Dirk.Fasshauer@unil.ch.

This article contains supporting information online at www.pnas.org/lookup/suppl/doi:10.1073/pnas.1408254111/-/DCSupplemental.

a multisubunit tethering complex known as the homotypic fusion and protein sorting complex (25). Nevertheless, the structure of Vps33 is very similar to other SM protein types despite having low sequence similarity (23, 24). It would be surprising if such structures were not preserved to maintain similar molecular functions. This raises the question of whether there are missing pieces to our understanding of the molecular role of SM proteins.

With the idea of a conserved molecular role of SM proteins in mind, we aimed here at a more thorough comparison of Sly1 and Munc18, which are still thought to represent two examples of SM proteins with contrasting syntaxin binding modes. So far nothing is known about a second binding site in the Sly1/Sed5 complex, but the presence of a homologous *N*-peptide binding site in Munc18 and Sly1 reveals a certain similarity of the two SM protein types. It is debated whether binding of Sly1 to the *N*-peptide of Sed5 is essential for Golgi trafficking while biochemically less is known (11, 26–28). Neither the effect of Sly1 on SNARE complex assembly has been determined rigorously, nor is it clear whether Sed5 can adopt a closed conformation that interferes with its ability to form a SNARE complex. We therefore sought to determine whether Sly1, in addition to its tight interaction with the *N*-peptide of Sed5, interacts with the remaining part of Sed5 and, if so, whether this interaction would have an impact on the ability of Sed5 to form a SNARE complex. We found that Sed5 adopts a closed conformation. Comparable to Munc18-1, Sly1 binds simultaneously to both the closed conformation and the *N*-peptide region of Sed5, although the latter is the major contributor to its affinity to the complex. Remarkably, in contrast to Munc18-1, which blocks SNARE complex assembly, Sly1 was found to assist Sed5 in forming a SNARE complex.

Results

Sed5 Adopts a Closed Conformation That Interferes with SNARE Complex Formation. Previous studies have shown that SNARE complex formation is generally accompanied by large structural changes (e.g., refs. 29, 30). When we mixed the four SNARE motifs of the ER–Golgi SNARE complex at 2 μM each (Sed5, Bos1, Bet1, and Sec22) (31–34), a major but slow increase in α-helical structure was observed by CD spectroscopy, indicating that they form a four-helix bundle complex (*SI Appendix*, Fig. S1). Although CD spectroscopy allowed us to follow SNARE complex formation of the SNARE motifs, it turned out that this approach was not suited for studying the activity of the entire cytoplasmic region of Sed5, which contains a well-folded three-helix bundle structure, the Habc domain (11) (Fig. 1*A*). In several other syntaxins, the Habc domain binds reversibly to the SNARE motif, resulting in a closed conformation (Fig. 1*B*) that interferes with SNARE complex formation (18, 30). Earlier studies had indicated that Sed5 adopts a closed conformation as well (27, 34, 35). To appraise the potency of the built-in open–closed switch in Sed5, we developed a fluorescence-based SNARE assembly assay. Using this approach, SNARE complex formation was observed as an increase in fluorescence anisotropy. As shown in Fig. 1*C*, the assembly of the ER–Golgi SNARE complex was slowed down drastically when the entire cytoplasmic region of Sed5 (Sed5 1–320) was used instead of its SNARE motif (Sed5 211–320), suggesting that cytoplasmic Sed5 adopts an autoinhibitory closed conformation that precludes SNARE complex formation, whereas its SNARE motif alone is not restricted. Interestingly, when we mixed the Habc domain and the SNARE motif of a split Sed5, SNARE assembly was slowed down (Fig. 1*C*), suggesting that the Habc domain binds to the SNARE motif in trans and inhibits its ability to engage the other members of the complex.

Next, we tested more directly whether Sed5 adopts a closed conformation. Upon size exclusion chromatography, a stoichiometric mix of the Habc domain (Sed5 1–210; i.e., including the *N*-peptide) and the SNARE motif comigrated (Fig. 1*D*), supporting the idea that the individual domains of a split Sed5 can

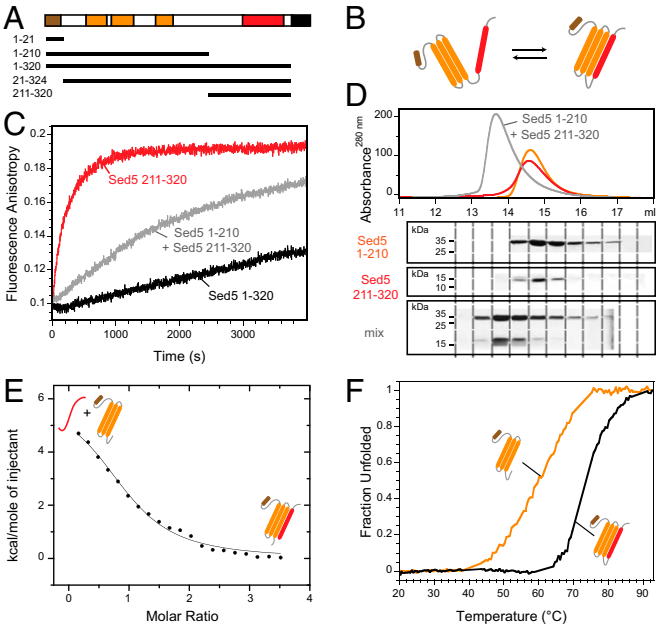

Fig. 1. Sed5 adopts a closed conformation. (*A*) Schematic drawing of the domain structure of Sed5 and fragments used in this study. The short *N*-peptide motif and the Habc helices (11) are shown in brown and orange colors, respectively, whereas the SNARE motif is colored in red. The transmembrane region is colored in black. (*A*, *Lower*) Sed5 variants used in this study are displayed. (*B*) Cartoon showing the conformational switch between open and closed conformation of syntaxins. In the closed conformation (*Right*), the SNARE motif (red) is bound to the Habc domain (orange), rendering it inaccessible to its SNARE partners. In the open conformation (*Left*), the SNARE motif is released from the Habc domain and is therefore free to form a SNARE complex. (*C*) SNARE complex formation was followed by the increase in fluorescence anisotropy of about 400 nM OG-labeled Sec22 126–186$^{C131\text{-}OG}$ upon mixing with 7 μM Bet1 1–118, Bos1 151–221, and full-length Sed5 (Sed5 1–320; black) or the SNARE motif of Sed5 (Sed5 211–320) in the absence (red) or presence of 28 μM of the isolated Habc domain (Sed5 1–210; gray). (*D*) Size exclusion chromatographic elution profiles for the individual Habc domain (Sed5 1–210) in orange, the individual SNARE motif (Sed5 211–320) in red, or the combined Sed5 fragments in gray (35 μM each). Prior to separation on a Superdex 200 column, the proteins were incubated overnight. The Habc domain comigrates with the SNARE motif. The respective peak fractions were analyzed by SDS/PAGE and stained with Coomassie Blue. Note that the interaction in trans can be observed by native gel electrophoreses as well (*SI Appendix*, Fig. S2). (*E*) Binding of the isolated Habc domain to the SNARE motif of Sed5 measured by ITC. Sed5 1–210 at 150 μM was titrated into 10 μM of Sed5 211–310. Shown are the integrated areas normalized to the amount of the Habc domain (kcal/mole) versus the molar ratio of the Habc domain to the SNARE motif. The solid curve is the best fit to the data for a single-site binding model using a nonlinear least squares fit. An endothermic interaction was observed upon titration, implying that folding of Sed5 into a closed conformation is entropy-driven. (*F*) Thermal CD melting curves of the entire cytoplasmatic domain (Sed5 1–320, black) and the Habc domain (Sed5 1–210, orange) of Sed5. The construct including the SNARE motif is about 10 °C more stable that the one lacking this domain.

form a complex in trans. The affinity of this interaction within a split Sed5 molecule was determined to be 2.7 μM by isothermal titration calorimetry (ITC; Fig. 1*E*). Finally, a comparison of CD thermal melting curves demonstrated that the Habc domain is drastically stabilized in the presence of the SNARE motif in the intact Sed5 molecule (Fig. 1*F*), in which the effective concentration of the two domains is much higher. These results are similar to the ones obtained for the secretory yeast syntaxin Sso1 (36), which resides in a rigid closed conformation (37) that slows SNARE complex formation by three orders of magnitude (30). Altogether, our results suggest that

Sed5 also adopts a rigid closed conformation that slows SNARE complex formation drastically.

Sly1 Accelerates SNARE Complex Assembly. The interaction of Sly1 with the *N*-peptide does not hinder SNARE complex assembly of Sly1-bound Sed5 (28), but the precise role of Sly1 during SNARE complex formation is still an open question. When we added Sly1 to our assay, we found that Sly1 substantially accelerates SNARE complex formation (Fig. 2*A*). This suggests that Sly1 must be able to control the reactivity of Sed5. As Sly1 does not accelerate SNARE assembly of the isolated SNARE motif of Sed5 (*SI Appendix*, Fig. S3), it is likely that Sly1 might be influencing the equilibrium between the open and closed conformation of Sed5. In whatever way Sly1 achieves this feat, our finding indicates that the interaction between Sly1 and Sed5 is not restricted to the *N*-peptide region of Sed5. The currently discussed modes of interaction between SM proteins and syntaxins are depicted in Fig. 2*B*. It should be noted that, although the crystal structure of the Sly1/Sed5 complex only contains the *N*-peptide region of Sed5 (12), it does not rule out that other regions interact as well. Such interaction may be weak and transient. In view of the fact that two other types of SM proteins, Munc18 and Vps45, interact with two spatially separated sites of their cognate syntaxins (15), we next probed the interaction mode of Sly1 and Sed5 in more detail.

Sly1 Interacts Not Only with the *N*-Peptide But Also with the Remainder of Sed5. To determine whether Sly1 also interacts with an additional site in Sed5, we first used ITC, an experimental strategy that had helped us before to shed new light on the binding mode of the SM proteins Munc18 and Vps45 (15). We observed that the isolated *N*-peptide (Sed5 1–21) binds to Sly1 with a favorable enthalpy ($\Delta H \sim -16$ kcal/mol) and a dissociation constant of ~1.5 nM (Fig. 2*C*). As anticipated, no binding was observed when the *N*-peptide region was removed (Sed5 21–324). Binding of Sed5 21–324 could not be restored when the *N*-peptide was added in trans (*SI Appendix*, Fig. S4). We also found that the isolated SNARE motif of Sed5 (Sed5 211–320) did not bind to Sly1 (*SI Appendix*, Fig. S3). Together, this confirms that the *N*-peptide is sufficient and necessary for high-affinity binding (10, 11).

When a Sed5 construct was used that contained the *N*-peptide and the adjacent Habc domain (Sed5 1–210), a small decrease in enthalpy was detected (~ −18 kcal/mole) (Fig. 2*C*). A more pronounced decrease in enthalpy was observed when the entire cytoplasmic region of Sed5 (Sed5 1–320)—that is, a construct that also included the SNARE motif—was used (~ −25.6 kcal/mole) (Fig. 2*C*). The difference in binding enthalpy likely reflects the contribution of additional binding surface to the interaction, suggesting that Sly1 indeed interacts with an additional part of Sed5.

We then further examined the notion that Sly1 makes use of two binding sites in Sed5 by introducing disruptive point mutations in each of the two respective regions of Sed5, the *N*-peptide and the SNARE motif. One substitution, F10A, was introduced into the *N*-peptide region of Sed5. This conserved phenylalanine binds into a hydrophobic pocket in domain 1 of Sly1 (12), and the mutation had been previously shown to disrupt binding to Sly1 (28). Indeed, when the point mutation was introduced into the isolated *N*-peptide (Sed5 1–21^{F10A}), no binding to Sly1 was detected (Fig. 2*D*). Interestingly, the point mutation did not prevent binding of the entire cytoplasmic region of Sed5 (Sed5 1–320^{F10A}), but greatly reduced the affinity to ~234 nM (Fig. 2*D*). This indicates that the remainder of Sed5 must indeed contribute to the overall binding strength. The other substitution was introduced into the SNARE motif of Sed5 at position 290 (Sed5 1–320^{I290A}). It is homologous to a mutation in the SNARE motif of syntaxin 1a that significantly interferes with binding of the closed conformation into the cavity of Munc18-1 (15). We found that this point mutation increased the enthalpy (*SI Appendix*, Table S1 and Fig. S4), suggesting that the mutated region of Sed5 is involved in binding to Sly1.

In summary, the ITC experiments confirm that Sly1 interacts tightly with Sed5. They also reveal that the *N*-peptide region is the major contributor to the high-affinity interaction, whereas the remainder of Sed5, possibly in a closed conformation, contributes an additional binding surface that only moderately increases the overall affinity of the Sly1/Sed5 complex.

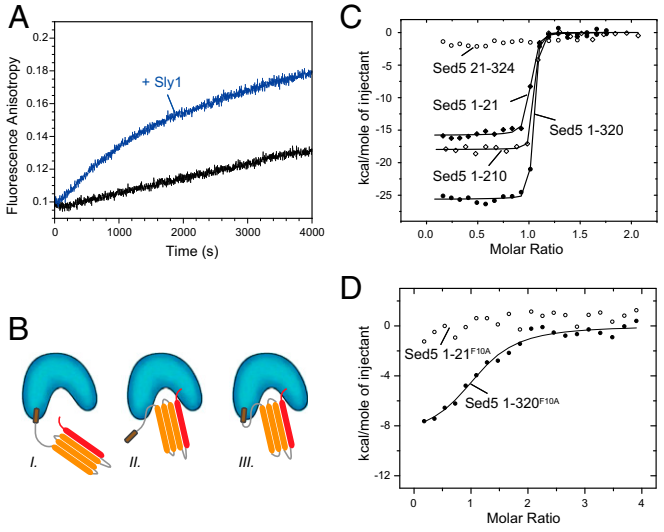

Fig. 2. Sly1 interacts with the *N*-peptide motif and with the remaining portion of Sed5. (*A*) Addition of Sly1 (11 μM) accelerates SNARE complex formation in the presence of Sed5 (Sed5 1–320, 7 μM, blue). SNARE complex formation was monitored by the increase in fluorescence anisotropy of fluorescent Sec22 126–186$^{C131\text{-}OG}$, as described in Fig. 1*C*. Note that the experiment in the absence of Sly1 (black) is the same as in Fig. 1*C*. Sly1 had no effect on the assembly rate when only the SNARE motif of Sed5 was used (*SI Appendix*, Fig. S3). Note that the acceleration observed agrees with the finding that the ER–Golgi SNAREs fuse liposomes only in the presence of Sly1 (48). (*B*) Representation of three different SM–syntaxin binding modes: involving solely the *N*-peptide (*I*), solely the closed conformation of the syntaxin (*II*), or the *N*-peptide and the closed conformation together (*III*). The SM protein is depicted in blue, whereas syntaxin is colored as in Fig. 1*B*. (*C*) Calorimetric titrations of truncated Sed5 variants Sed5 1–21 (15 μM), Sed5 1–210 (15 μM), Sed5 1–320 (15 μM), and Sed5 21–324 (30 μM) into Sly1 (2 μM). (*D*) Calorimetric titrations of the Sed5 mutants Sed5 1–21^{F10A} (25 μM) and Sed5 1–320^{F10A} (25 μM) into Sly1 (1.5 μM). Note that all ITC experiments are shown in *SI Appendix*, Fig. S4 and that the corresponding data are given in *SI Appendix*, Table S1.

Sly1 Rearranges the Closed Conformation of Sed5. If we are correct and Sly1 does indeed bind to the remainder of Sed5 in a closed conformation, where the SNARE motif is tightly bound to the Habc domain, why does Sly1 then not inhibit SNARE complex formation in a similar fashion as Munc18? To address this question, we made use of the fact that the two domains of Sed5, the Habc domain (Sed5 1–210) and the SNARE motif (Sed5 211–320), form a stable complex that comigrates upon gel filtration (Fig. 1*D*). We also observed that a complex between Sly1 and Sed5 1–210 comigrates. However, when Sly1 was combined with both regions of a split Sed5, the Habc domain and the SNARE motif, only Sly1 and the Habc domain comigrated, whereas the SNARE motif eluted later (Fig. 3*A*). This suggests that in the presence of Sly1, the SNARE motif of Sed5 is less tightly bound to the Habc domain.

To more directly test whether the SNARE motif is less tightly bound in the presence of Sly1, we first compared the dissociation rates of different Sed5 fragments from Sly1. For this, we labeled different Sed5 fragments with a fluorescent dye. Upon addition of Sly1, the fluorescence anisotropy of each of the labeled Sed5 molecules rapidly increased. We then determined the off-rates of the different Sly1/Sed5 complexes by competitive dissociation

(Fig. 3*B*). As expected, the sole *N*-peptide dissociated more quickly than the longer Sed5 fragments (Sed5 1–21, 0.00114 s^{-1} vs. Sed5 1–210, 0.00021 s^{-1} and Sed5 1–320, 0.00042 s^{-1}), corroborating the results obtained by ITC experiments shown above (Fig. 2), which indicated that the remainder of Sed5 contributes to the strength of the interaction. An even more surprising conclusion that can be drawn from the off-rate experiments is the fact that the grip of Sly1 on Sed5 is moderately loosened in the presence of the SNARE motif, as a construct comprising the *N*-peptide region and Habc domain (Sed5 1–210) dissociated more slowly than the intact cytoplasmic portion of Sed5. One possible explanation for this result is that the configuration of the SNARE motif in the Sly1/Sed5 complex is different from that in individual Sed5.

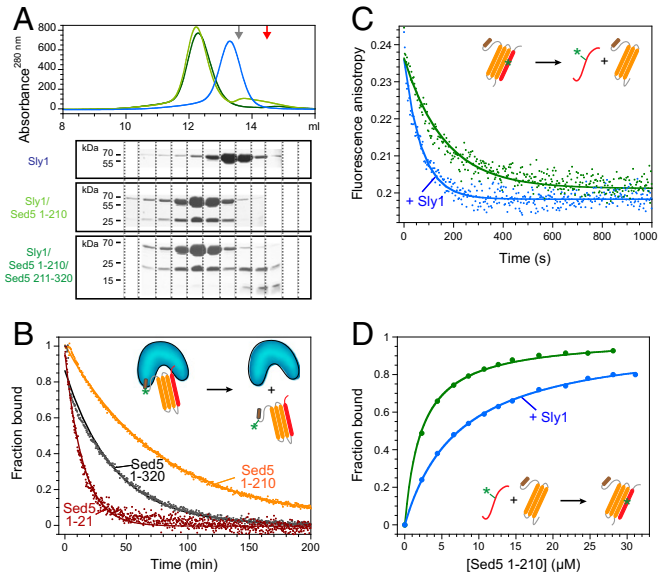

Fig. 3. Sly1 accelerates SNARE complex formation by loosening the closed conformation of Sed5. (*A*) Size exclusion chromatographic elution profiles for Sly1 (blue), the combination of Sly1 and the Habc domain of Sed5 (Sed5 1–210, dark green), and the combination of Sly1, Habc domain, and SNARE motif of Sed5 (Sed5 211–320, light green). Arrows indicate the peak maxima of the individual SNARE motif of Sed5 (red) and of the combination of the Habc domain and SNARE motif of Sed5 (gray) as shown Fig. 1*D*. In the presence of Sly1, the SNARE motif of Sed5 dissociates from the Habc domain. Note that a portion of the Habc domain not bound to Sly1 still interacts with the SNARE motif. The peak fractions were analyzed by SDS/PAGE and stained with Coomassie Blue. Results of the analogous experiment with combinations of Sly1 and Sed5 1–320 or Sed5 211–320 are shown in *SI Appendix*, Fig. S5. (*B*) Determination of the off-rates of different Sly1/Sed5 complexes by competitive dissociation. The anisotropy signal is reported as a fraction of bound fluorescent molecules. The dissociation was fit by a single exponential: Sed5 1–21, dark red curve; Sed5 1–210, orange curve; Sed5 1–320, black curve. The dissociation rate of the *N*-peptide did not change when Sed5 21–324 was added in trans (*SI Appendix*, Fig. S6). (*C*) The dissociation rate of the Habc/SNARE motif complex was determined by rapid dilution. In the absence of Sly1, the rate was ~0.006 s^{-1}. In the presence of 32 μM Sly1, the rate was ~0.014 s^{-1}. Thus, Sly1 accelerates the off-rate of a split Sed5. (*D*) Complex formation between the individual domains of Sed5 leads to an increase of fluorescence anisotropy of a labeled SNARE motif (Sed5 211–320$^{C278\text{-}TR}$) when mixed with the Habc domain. To determine the effect of Sly1 on the affinity between both Sed5 segments, ~100 nM of labeled SNARE motif was incubated with increasing amounts of the Habc domain in the presence or absence of about 30 μM Sly1. The anisotropy signal is reported as a fraction of bound fluorescent molecules. Binding curves were fitted using nonlinear regression to determine the affinities between the Habc domain and the SNARE motif of Sed5. The K_d was about threefold lower in the presence of Sly1 (K_d ~ 7.3 μM) than in its absence (K_d ~ 2.3 μM). Note that the affinity determined by fluorescence anisotropy agrees well with the one obtained by ITC (K_d ~ 2.7 μM; *SI Appendix*, Table S1).

To observe the influence of Sly1 on the state of the SNARE motif more directly, we next labeled the SNARE motif with a fluorescent dye (Sed5$^{C278\text{-}TR}$ 211–320). The fluorescence anisotropy of the labeled SNARE domain increased upon complex formation with the Habc domain. We then determined the off-rate of the Habc domain/SNARE motif complex by rapid dilution. When the experiment was carried out in the presence of Sly1, the SNARE motif dissociated more rapidly (Fig. 3*C*). Correspondingly, a titration approach confirmed that the SNARE motif is less tightly bound in the presence of Sly1 (Fig. 3*D*).

In summary, the results substantiate the hypothesis that binding of Sly1 to Sed5 alters the configuration of the SNARE motif, maybe indirectly through a conformational change in the Habc domain, so that it can participate in SNARE complex formation.

Discussion

SNARE and the SM protein families are key for the docking and fusion of transport vesicles with their respective target membrane. Numerous genetic studies have provided compelling evidence that SM proteins act primarily through one subgroup of SNARE proteins, the syntaxins (6, 7). For instance, the secretory SM protein Munc18 forms a tight complex with syntaxin 1, whereas Sly1 interacts tightly with the syntaxin Sed5. Naturally, it was assumed that these homologous factors share a common molecular mechanism. However, this view received less support when the structures of their high-affinity complexes revealed them to be in apparently different binding modes. Munc18-1 was found to clasp around a major portion of syntaxin 1a in a closed conformation (18), whereas Sly1 interacts with the *N*-peptide of Sed5 (12). Later it was shown that Munc18-1 also binds simultaneously to the *N*-peptide of syntaxin 1a, although with much less affinity (15, 20). Here, we provide strong evidence that Sly1 not only binds to the *N*-peptide of Sed5 but also is able to interact with the remainder of Sed5.

Our findings confirm that a conformational switch between a closed and an open conformation is at the heart of syntaxin's function (38). Notably, we observed that Sed5 adopts a more rigid closed conformation than syntaxin 1a. For both syntaxins, the Habc domain accounts for a slower SNARE assembly, because in its absence the assembly proceeds faster. However, whereas syntaxin 1a is slowed only by a factor of approximately 10 (39), the assembly speed of Sed5 is reduced by three orders of magnitude. Possibly, Sed5 requires more assistance than syntaxin 1a to be released from its autoinhibitory state into a state that is required for the interaction with its SNARE partners.

Our results corroborate the idea that a binding mode with two spatially separated binding sites allows an SM protein to control the conformational switch of the bound syntaxin. However, why do SM proteins use two different binding sites for this purpose? One possibility is that the two binding sites are allosterically coupled to control the accessibility of the bound syntaxin (40, 41). It is also possible, although not exclusive, that the two binding sites represent consecutive steps of a reaction cascade or handover mechanism controlled by the SM protein. It is likely that an interaction with the remote *N*-peptide region of syntaxin does not have a direct impact on the ability of syntaxin to engage in SNARE interactions. Rather, the *N*-peptide might serve as an anchor point to steer the SM protein toward the membrane fusion site, where it can liberate the SNARE motif of syntaxin and act on the assembling SNARE complex or even on the lipid bilayers (11, 12, 21, 42).

A noticeable difference between the two SM protein–syntaxin complexes is that the relative energetic contribution of each binding site is reversed: Whereas the *N*-peptide of Sed5 binds with nanomolar affinity to Sly1, the *N*-peptide of syntaxin 1a binds with ~1,000 times lower affinity. Point mutations that interfere with the binding of the *N*-peptide to Sly1 have been shown not to interfere in ER–Golgi transport (28). This puzzling result can now be explained in light of our finding that the remainder of Sed5 also contributes to the interaction. In other words, despite the impeding point mutations, the two proteins

were still able to form a complex, albeit with less affinity. Apparently this affinity is sufficient to maintain the overall function of the protein complex. Analogous experiments have been performed to explore the role of the *N*-peptide binding site of Munc18-1. Point mutations in Munc18-1 were shown to strongly interfere with binding of the *N*-peptide; however, the mutants were still able to rescue synaptic secretion in Munc18-1 knockout neurons (43). Conversely, a syntaxin 1a, in which the *N*-peptide had been removed, was not able to rescue synaptic secretion in syntaxin-deficient neurons (44). The stark difference between the two studies may be explained by the fact that both binding sites are crucial for the function of the complex. The point mutations in Munc18-1 used in one study may have weakened only one interaction site. It seems feasible that this local defect could be overcome, as both binding sites act together. By contrast, in the study by Zhou et al. (44), a syntaxin variant was used in which one binding region had been deleted altogether, a deficiency that might not be able to be overcome by the secretion apparatus. Note that comparable results were obtained for *Caenorhabditis elegans* (42, 45, 46).

Although the *N*-peptide interaction mode of the two SM protein/syntaxin complexes exhibits nuanced differences, the results of the interaction with the remainder of syntaxin appear to be diametrically opposed: Whereas Munc18-1 interferes with the ability of the bound syntaxin to form a SNARE complex, Sly1 assists Sed5 in binding to its partner SNAREs. In fact, if one ignored the inhibitory activity of Munc18-1, Sly1's stimulating effect would almost perfectly fit the job description of SM proteins derived from various in vivo studies. However, how can the different outcomes be explained? This question cannot yet be answered sufficiently, because many of the details appear to be missing. However, one can obtain an initial impression by taking a closer look at the fundamental role of SM proteins. It is generally thought that SM proteins orchestrate the zippering of the SNARE proteins of fusing membranes, primarily by shaping the conformation of the bound syntaxin. To alter the activity of the bound syntaxin, an SM protein must be able to directly or indirectly act on the SNARE motif that is attached to the Habc domain. In the Munc18-1/syntaxin complex, the SNARE motif is clamped securely in the cavity of Munc18-1, a conformation that impedes syntaxin's ability to form a SNARE complex (15). The structure of the interaction of Sly1 with the remainder of Sed5 is not currently known, but because Sly1 does not interfere with but strongly supports Sed5's activity, we can safely assume that the complex resides in a somewhat different conformation, a scenario depicted in Fig. 4. In fact, our data using the isolated domains of Sed5 suggest that the SNARE motif of Sed5 is less tightly coupled to its Habc domain in complex with Sly1 than as in the individual Sed5. By contrast, Munc18-1 stabilizes the interaction between the domains of a split syntaxin 1a (15). It is possible that during the reaction, a transition state complex is formed between the SM protein and syntaxin. In the case of Sly1 and Sed5, the lower activation energy leads, as expected, to a faster reaction. In the case of Munc18-1 and syntaxin 1a, it is possible that the complex formed does not represent the transition state complex but rather a stable configuration from which syntaxin cannot escape. The stable configuration might allow Munc18 to control syntaxin's accessibility, a property that is well suited for tight regulation of exocytosis. Possibly, the Munc18/syntaxin complex might subsequently, with the help of other factors like the protein Munc13 (47), switch to the transition state configuration. In this regard, it should be noted that mutations in the linker region—that is, the "LE mutations" (19)—of syntaxin can overcome this block without the aid of other factors (15, 47) and without interfering strongly with the global conformation of the Munc18-1/syntaxin complex (41). If the above outlined scenario is correct, these findings indicate that the energy barrier between the putative stable intermediate and transition state configuration might be relatively small.

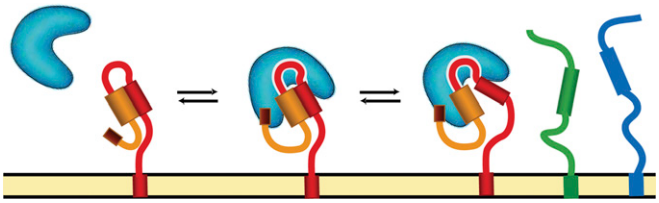

Fig. 4. Model of how Sly1 facilitates assembly of ER–Golgi SNAREs. Whereas individual Sed5 (colored as in Fig. 1*A*) resides predominantly in a closed conformation, it is rendered more open by Sly1 (blue). The SNARE motif of Sly1-bound Sed5 is less tightly bound and can interact with other ER–Golgi SNAREs (e.g., Bos1, green; Sec22, dark blue).

In summary, our findings suggest that Sly1 makes use of two binding sites to prepare Sed5 for SNARE complex assembly. Most likely, the *N*-peptide binding site serves to keep Sly1 at the relevant position, whereas the other interaction site serves to act on the conformation of syntaxin. On a structural level, however, it remains to be clarified how exactly Sly1 renders Sed5 more open for its SNARE partners. Moreover, it remains unclear whether Sly1's role is only to present an open Sed5 to the partner SNAREs or whether it also subsequently facilitates the assembly of the SNARE complex. Our data corroborate the idea that SM proteins and syntaxins originally shared a common molecular mechanism that involved two spatially separated binding sites. Because then, different homologous pairs have diverged, although to different degrees, so that their commonalities are barely discernible.

Experimental Procedures

Protein Constructs. Apart from the expression constructs for yeast Sly1 1–666 in pGEX-TT vector and Bet1 1–118 in pET19b vector, each of the recombinant proteins was cloned into a pET28a vector, which contains an N-terminal, thrombin-cleavable His_6-tag. The constructs for Sly1 1–666, Sed5 21–324, Bet1 1–118, and Sec22 126–186 (13, 28) were kindly provided by R. Peng (University of Bern, Bern, Switzerland). The following truncated variants of Sed5 were generated in this study—Sed5 1–210, Sed5 1–320, and Sed5 211–320—as were the Sed5 1–320 constructs containing the point mutations F10A and I290A. The following single-cysteine variants—Sed5 1–210^{K22C}, Sed5 1–320^{K22C}, Sed5 211–320^{S278C}, and Sec22 126–186^{D131C}—were generated for fluorescence measurements. The construct encoding for the SNARE motif of Bos1 (Bos1 151–221) was also newly generated in this study. The peptides corresponding to the *N*-peptide regions of Sed5 (Sed5 1–21) and Ufe1 (Ufe1 1–21) were synthesized by Biosyntan GmbH, as were the variants containing the single-point mutation Sed5 1–21^{F10A} and Sed5 1–21 with a C-terminal cysteine.

Protein Purification. All proteins were expressed in the *Escherichia coli* strain BL21 (DE3) and, except Sly1, purified by Ni^{2+}-nitrilotriacetic acid chromatography followed by ion exchange chromatography on an Äkta system (GE Healthcare). The proteins were eluted with a linear gradient of NaCl in 20 mM Tris, pH 7.4, 1 mM EDTA (standard buffer) as previously described (15). We added 1 mM DTT for proteins containing cysteine residues. His_6-tags were removed using thrombin. For the entire cytosolic portion of Sed5 (Sed5 1–320), ion exchange chromatography was performed in the presence of 2 M urea to prevent aggregation. Afterward, urea was removed by dialysis against standard buffer containing 200 mM NaCl, in which purified Sed5 was stable. Sly1 was first purified by GST affinity chromatography. The GST moiety was cleaved by thrombin on the beads. Sly1 was further purified by size exclusion chromatography on a Superdex-200 column in standard buffer containing 200 mM NaCl and 1 mM DTT. Quaternary SNARE complexes consisting of Sed5 (Sed5 211–320 or Sed5 1–320), Bos1 151–221, Bet1 1–118, and Sec22 126–186 were assembled from purified components and purified by ion exchange chromatography. Generally, the purity of the proteins was greater than 95% as determined by SDS/PAGE. Protein concentrations were determined by absorption at 280 nm.

ITC. ITC was performed on a VP-ITC instrument (GE Healthcare) at 25 °C as previously described (15). Proteins were dialyzed twice against PBS buffer (20 mM sodium phosphate, pH 7.4, 200 mM NaCl, 1 mM DTT) and degassed before experiments. Typically, titrations were carried out by 15-μL injections.

The baseline-corrected raw data were analyzed with MicroCal Origin 7.0 to obtain the binding enthalpy (ΔH), the stoichiometry (n), and the equilibrium association constant (K_a). Binding curves were generated by using a nonlinear least squares fit for a single-site binding model.

Fluorescence Spectroscopy. Fluorescence measurements were carried out in a Fluorolog 3 spectrometer in a T configuration equipped for polarization (model FL322; Horiba Jobin Yvon). Single-cysteine variants were labeled with Texas Red maleimide or Oregon Green (OG) 488 iodoacetamide according to the manufacturer's instructions (Invitrogen). The concentration of labeled proteins was determined by a Bradford assay. Experiments were performed at 25 °C in 1-cm, 0.4-cm, or ultramicro quartz cuvettes (Hellma) in a PBS buffer. Local flexibility of labeled residues, which increases upon complex formation and decreases upon dissociation, was reported in terms of fluorescence anisotropy (r) essentially as described (15). For affinity titrations, the signal was averaged for 2–3 min after each addition of unlabeled titrant. The signal change was normalized and reported as a fraction of bound fluorescent molecules. Binding constants were obtained from least squares fits to the equation: $r_{min} + (r_{max} - r_{min}) \times$ [Sed5 1–210]/([Sed5 1–210] + K_d). For the competitive dissociation experiments, ∼50 nM of OG-labeled Sed5 variants (Sed5 1–21$^{C22\text{-}OG488}$, 1–210 $^{C22\text{-}OG488}$, or 1–320 $^{C22\text{-}OG488}$) was first mixed with saturating amounts of Sly1 (∼300 nM). Then, an excess of unlabeled Sed5 variants (∼5 μM) was added, and the decrease in fluorescence anisotropy was followed. For the rapid dilution experiments, ∼60 nM of the labeled SNARE motif was mixed with 22 μM of Habc domain in a total volume of 100 μL. Then, the mixture was rapidly diluted to 3 mL, and the dissociation was monitored by the decrease in fluorescence anisotropy.

CD Spectroscopy. Measurements were carried out in PBS buffer as previously described (29) using a Chirascan instrument (Applied Photophysics). Spectra were recorded in quartz cuvettes with a path length of 0.1 cm. For thermal denaturations, the ellipticity at 222 nm was recorded between 20 and 95 °C at a temperature increment of 30 °C/h. Kinetic measurements were carried out using 1-cm quartz cuvettes at 25 °C. Proteins were mixed, and the change in the CD signal was followed at 222 nm.

ACKNOWLEDGMENTS. We thank Wolfgang Berning-Koch for technical assistance; Hans Dieter Schmitt, Javier Matias Hernandez, and Geert van den Bogaart for helpful discussions; and Gregory Kabachinski for a critical reading of the manuscript. F.E.D. was supported by a fellowship of the Göttingen Graduate School for Neurosciences and Molecular Biosciences.

1. Hardwick KG, Pelham HR (1992) SED5 encodes a 39-kD integral membrane protein required for vesicular transport between the ER and the Golgi complex. *J Cell Biol* 119(3):513–521.
2. Søgaard M, et al. (1994) A rab protein is required for the assembly of SNARE complexes in the docking of transport vesicles. *Cell* 78(6):937–948.
3. Hong W, Lev S (2014) Tethering the assembly of SNARE complexes. *Trends Cell Biol* 24(1):35–43.
4. Jahn R, Fasshauer D (2012) Molecular machines governing exocytosis of synaptic vesicles. *Nature* 490(7419):201–207.
5. Südhof TC, Rothman JE (2009) Membrane fusion: Grappling with SNARE and SM proteins. *Science* 323(5913):474–477.
6. Carr CM, Rizo J (2010) At the junction of SNARE and SM protein function. *Curr Opin Cell Biol* 22(4):488–495.
7. Toonen RF, Verhage M (2007) Munc18-1 in secretion: Lonely Munc joins SNARE team and takes control. *Trends Neurosci* 30(11):564–572.
8. Rizo J, Südhof TC (2012) The membrane fusion enigma: SNAREs, Sec1/Munc18 proteins, and their accomplices—Guilty as charged? *Annu Rev Cell Dev Biol* 28:279–308.
9. Grabowski R, Gallwitz D (1997) High-affinity binding of the yeast cis-Golgi t-SNARE, Sed5p, to wild-type and mutant Sly1p, a modulator of transport vesicle docking. *FEBS Lett* 411(2-3):169–172.
10. Kosodo Y, Noda Y, Yoda K (1998) Protein-protein interactions of the yeast Golgi t-SNARE Sed5 protein distinct from its neural plasma membrane cognate syntaxin 1. *Biochem Biophys Res Commun* 250(2):212–216.
11. Yamaguchi T, et al. (2002) Sly1 binds to Golgi and ER syntaxins via a conserved N-terminal peptide motif. *Dev Cell* 2(3):295–305.
12. Bracher A, Weissenhorn W (2002) Structural basis for the Golgi membrane recruitment of Sly1p by Sed5p. *EMBO J* 21(22):6114–6124.
13. Peng R, Gallwitz D (2002) Sly1 protein bound to Golgi syntaxin Sed5p allows assembly and contributes to specificity of SNARE fusion complexes. *J Cell Biol* 157(4):645–655.
14. Carr CM, Grote E, Munson M, Hughson FM, Novick PJ (1999) Sec1p binds to SNARE complexes and concentrates at sites of secretion. *J Cell Biol* 146(2):333–344.
15. Burkhardt P, Hattendorf DA, Weis WI, Fasshauer D (2008) Munc18a controls SNARE assembly through its interaction with the syntaxin N-peptide. *EMBO J* 27(7):923–933.
16. Yang B, et al. (1999) SNARE interactions are not selective. Implications for membrane fusion specificity. *J Biol Chem* 274(9):5649–5653.
17. Verhage M, et al. (2000) Synaptic assembly of the brain in the absence of neurotransmitter secretion. *Science* 287(5454):864–869.
18. Misura KM, Scheller RH, Weis WI (2000) Three-dimensional structure of the neuronal-Sec1-syntaxin 1a complex. *Nature* 404(6776):355–362.
19. Dulubova I, et al. (1999) A conformational switch in syntaxin during exocytosis: Role of munc18. *EMBO J* 18(16):4372–4382.
20. Burkhardt P, et al. (2011) Primordial neurosecretory apparatus identified in the choanoflagellate Monosiga brevicollis. *Proc Natl Acad Sci USA* 108(37):15264–15269.
21. Dulubova I, et al. (2002) How Tlg2p/syntaxin 16 'snares' Vps45. *EMBO J* 21(14):3620–3631.
22. Furgason ML, et al. (2009) The N-terminal peptide of the syntaxin Tlg2p modulates binding of its closed conformation to Vps45p. *Proc Natl Acad Sci USA* 106(34):14303–14308.
23. Baker RW, Jeffrey PD, Hughson FM (2013) Crystal structures of the Sec1/Munc18 (SM) protein Vps33, alone and bound to the homotypic fusion and vacuolar protein sorting (HOPS) subunit Vps16*. *PLoS ONE* 8(6):e67409.
24. Graham SC, et al. (2013) Structural basis of Vps33A recruitment to the human HOPS complex by Vps16. *Proc Natl Acad Sci USA* 110(33):13345–13350.
25. Rieder SE, Emr SD (1997) A novel RING finger protein complex essential for a late step in protein transport to the yeast vacuole. *Mol Biol Cell* 8(11):2307–2327.
26. Dulubova I, et al. (2003) Convergence and divergence in the mechanism of SNARE binding by Sec1/Munc18-like proteins. *Proc Natl Acad Sci USA* 100(1):32–37.
27. Williams AL, Ehm S, Jacobson NC, Xu D, Hay JC (2004) rsly1 binding to syntaxin 5 is required for endoplasmic reticulum-to-Golgi transport but does not promote SNARE motif accessibility. *Mol Biol Cell* 15(1):162–175.
28. Peng R, Gallwitz D (2004) Multiple SNARE interactions of an SM protein: Sed5p/Sly1p binding is dispensable for transport. *EMBO J* 23(20):3939–3949.
29. Fasshauer D, Otto H, Eliason WK, Jahn R, Brünger AT (1997) Structural changes are associated with soluble N-ethylmaleimide-sensitive fusion protein attachment protein receptor complex formation. *J Biol Chem* 272(44):28036–28041.
30. Nicholson KL, et al. (1998) Regulation of SNARE complex assembly by an N-terminal domain of the t-SNARE Sso1p. *Nat Struct Biol* 5(9):793–802.
31. Flanagan JJ, Barlowe C (2006) Cysteine-disulfide cross-linking to monitor SNARE complex assembly during endoplasmic reticulum-Golgi transport. *J Biol Chem* 281(4):2281–2288.
32. Joglekar AP, Xu D, Rigotti DJ, Fairman R, Hay JC (2003) The SNARE motif contributes to rbet1 intracellular targeting and dynamics independently of SNARE interactions. *J Biol Chem* 278(16):14121–14133.
33. Tsui MM, Tai WC, Banfield DK (2001) Selective formation of Sed5p-containing SNARE complexes is mediated by combinatorial binding interactions. *Mol Biol Cell* 12(3):521–538.
34. Xu D, Joglekar AP, Williams AL, Hay JC (2000) Subunit structure of a mammalian ER/Golgi SNARE complex. *J Biol Chem* 275(50):39631–39639.
35. Mossessova E, Bickford LC, Goldberg J (2003) SNARE selectivity of the COPII coat. *Cell* 114(4):483–495.
36. Fiebig KM, Rice LM, Pollock E, Brunger AT (1999) Folding intermediates of SNARE complex assembly. *Nat Struct Biol* 6(2):117–123.
37. Munson M, Chen X, Cocina AE, Schultz SM, Hughson FM (2000) Interactions within the yeast t-SNARE Sso1p that control SNARE complex assembly. *Nat Struct Biol* 7(10):894–902.
38. MacDonald C, Munson M, Bryant NJ (2010) Autoinhibition of SNARE complex assembly by a conformational switch represents a conserved feature of syntaxins. *Biochem Soc Trans* 38(Pt 1):209–212.
39. Margittai M, et al. (2003) Single-molecule fluorescence resonance energy transfer reveals a dynamic equilibrium between closed and open conformations of syntaxin 1. *Proc Natl Acad Sci USA* 100(26):15516–15521.
40. Dawidowski D, Cafiso DS (2013) Allosteric control of syntaxin 1a by Munc18-1: Characterization of the open and closed conformations of syntaxin. *Biophys J* 104(7):1585–1594.
41. Colbert KN, et al. (2013) Syntaxin1a variants lacking an N-peptide or bearing the LE mutation bind to Munc18a in a closed conformation. *Proc Natl Acad Sci USA* 110(31):12637–12642.
42. Rathore SS, et al. (2010) Syntaxin N-terminal peptide motif is an initiation factor for the assembly of the SNARE-Sec1/Munc18 membrane fusion complex. *Proc Natl Acad Sci USA* 107(52):22399–22406.
43. Meijer M, et al. (2012) Munc18-1 mutations that strongly impair SNARE-complex binding support normal synaptic transmission. *EMBO J* 31(9):2156–2168.
44. Zhou P, et al. (2013) Syntaxin-1 N-peptide and Habc-domain perform distinct essential functions in synaptic vesicle fusion. *EMBO J* 32(1):159–171.
45. McEwen JM, Kaplan JM (2008) UNC-18 promotes both the anterograde trafficking and synaptic function of syntaxin. *Mol Biol Cell* 19(9):3836–3846.
46. Johnson JR, et al. (2009) Binding of UNC-18 to the N-terminus of syntaxin is essential for neurotransmission in Caenorhabditis elegans. *Biochem J* 418(1):73–80.
47. Ma C, Li W, Xu Y, Rizo J (2011) Munc13 mediates the transition from the closed syntaxin-Munc18 complex to the SNARE complex. *Nat Struct Mol Biol* 18(5):542–549.
48. Furukawa N, Mima J (2014) Multiple and distinct strategies of yeast SNAREs to confer the specificity of membrane fusion. *Sci Rep* 4:4277.

Supporting Information Demircioglu et al.

Fig. S1: Assembly of ER-Golgi SNARE components monitored by CD spectroscopy.

A. Structural change upon SNARE complex formation. CD spectra were collected either from single SNARE motifs (5 μM from each of Sed5 211-320 (Qa-), Bos1 51-221 (Qb-), Bet1 1-118 (Qc-) and Sec22 126-186 (R-SNARE) (1-5)) or after their overnight incubation in equimolar amounts. The CD spectrum shown in dashed line is the theoretical non-interacting spectrum, calculated from the observed CD spectra of the SNARE segments. The spectrum of the quaternary complex formed between SNARE segments is shown in black.

B. Assembly kinetics of ER-Golgi SNAREs followed by CD spectroscopy**.** Assembly kinetics of ER-Golgi SNAREs was observed by monitoring the change in the mean residue ellipticity at 222 nm over time. The measurement was started after addition of 2 μM Sed5p 211-320 to an equimolar mixture of the other SNAREs (Bos1 151-221, Bet1 1-118, Sec22 126-186). SNARE complex assembly is slow (not completed after 8 hours at 2 μM of each subunit), roughly comparable to the speed of assembly of neuronal complex when SNAP-25 helices are used in two different constructs (6).

Fig. S2: Interaction between the Habc domain and the SNARE motif of Sed5 monitored by nondenaturing gel electrophoresis.

Prior to separation by nondenaturing gel electrophoresis, the isolated Habc domain (Sed5 1-210) and the SNARE motif of Sed5 (Sed5 211-320) were incubated overnight in standard buffer containing 200 mM NaCl. Constant amounts of the SNARE motif (31.4 μM) were mixed with increasing amounts of the Habc domain (concentrations as indicated). Note that due to an isoelectric point of 9.6, the individual Habc domain is not visible in the nondenaturing gel.

Fig. S3: Sly1 does not affect the assembly rate of the isolated SNARE motif of Sed5 with its partner SNAREs.

Addition of Sly1 (11 μM) has no effect on the rate of SNARE complex formation in the presence of the SNARE segment of Sed5 (Sed5 211-320, 7 μM). SNARE complex formation was monitored by the increase in fluorescence anisotropy of fluorescent Sec22 (Sec22 126-186$^{C131\text{-}OG}$) as described in Fig. 1C.

Fig. S4: Isothermal titration calorimetry experiments that have been performed in this study.

All isothermal titrations were performed at 25 °C in PBS buffer. In each plot, the top panel displays the base-line corrected raw data in power versus time. The lower panel shows the integrated areas normalized to the amount of the injectant (kcal mol^{-1}) versus its molar ratio to the macromolecule(s) in the cell. The solid lines represent the best fit to the data for a single-site binding model. Thermodynamic parameters calculated from the fits are given in Table S1. All experiments have been performed in replicates, and a representative example is shown.

In most experiments, 15 μM of the different Sed5 variants were injected into 2 μM of Sly1. For the titration of Sed5 21-324 30 μM were used, however. For the titration of Sed5 1-21^{F10A} and Sed5 1-320^{F10A} 25 μM were injected into 1.5 μM of Sly1. Moreover, 25 μM of the SNARE complex containing the SNARE motif of Sed5 (Sed5 211-320) was titrated into 3.3 μM Sly1, whereas the purified SNARE complex containing the entire cytosolic domain of Sed5 (Sed5 1-320) was injected into Sly1 at lower concentrations (7.5 μM and 1 μM, respectively), since it was difficult to purify this SNARE complex in larger amounts. In general, for variants and complexes for which we only detected small or no heat changes higher protein concentrations were used.

Because the precise determination of the binding affinity using ITC becomes progressively difficult once it approaches and surpasses the nanomolar range, we used displacement titration in order to more precisely determine the affinity of full-length Sed5. For this experiment, we needed to displace a known binding partner from Sly1 with

varying amounts of Sed5. For this, we chose the N-peptide of the syntaxin Ufe1, which is involved in retrograde vesicle trafficking and known to bind to Sly1 (7-9). Replacement titrations were performed according to (10). 20 μM Sed5 1-320 or 40 μM Sed5 1-210 were injected into Sly1 (2 μM)/ Ufe1 1-21 (15 μM) mixes. For fitting of the competitive binding experiments, thermodynamic parameters of Sly1 (2 μM)/ Ufe1 1-21 (15 μM) binding (N, K_d and ΔH) were used as input. Upon ITC, we determined an affinity of 35.4 nM and an enthalpy of - 15.8 kcal/mole for the interaction of Sly1 and the N-peptide of Ufe1. The difference in enthalpy between binding of Sly1 to Sed5 1-320 and to the N-peptide of Ufe1 enabled us to titrate Sed5 to a premix of Sly1 and the Ufe1 N-peptide. This experimental strategy revealed an affinity of ≈ 0.17 nM for the interaction of Sly1 and Sed5 1-320. Unfortunately, this strategy could not be used for shorter Sed5 fragments, because their binding enthalpies were almost identical to the one of the Ufe1 N-peptide.

Notice that an ITC experiment, in which a preformed complex between the Habc and the SNARE motif was titrated into Sly1, did not provide a definitive result as the determined enthalpy (≈ 22.7 kcal/mole) and affinity (0.48 nM) were in between the affinities obtained for the Habc and for the full-length Sed5 molecule. It needs to be stressed, however, that because these affinities were obtained at the resolution limit of the ITC instrument, they have to be treated with caution.

We also tested whether Sly1 binds to an assembled SNARE complex. For this, we purified quaternary complexes containing the SNARE motifs of Bos1, Bet1, Sec22 and either the entire cytoplasmic region of Sed5 (Sed5 1-320) or the SNARE motif of Sed5 (Sed5 211-320). We found that the SNARE complex containing Sed5 1-320 bound with an enthalpy and affinity comparable to Sed5 fragments containing the intact N-terminal region, whereas no binding of the SNARE complex containing only the SNARE motif of Sed5 could be detected. This suggests that Sly1 does not bind with significant affinity to the core region of the completely assembled ER-Golgi SNARE complex.

Fig. S5: Sly1 forms a complex with the entire cytosolic portion but not with the isolated SNARE motif of Sed5.

A. Size exclusion chromatography elution profiles of Sly1 in blue, the entire cytosolic portion of Sed5 (1-320) in black, and an equimolar mixture in dark blue (14 μM each). The Sly1/Sed5 complex elutes at a higher molecular mass than the two monomers.

B. Elution profiles of Sly1 in blue, the SNARE motif of Sed5 (211-320) in red and an equimolar mixture in pink (35 μM each). The respective peak fractions were analyzed by SDS-PAGE and stained with Coomassie Blue.

Fig. S6: The remainder of Sed5 does not affect the binding strength of the Sed5 N-peptide to Sly1.

As in Fig. 3C about 50 nM of Oregon Green-labeled N-peptide of Sed5 (Sed5 $1\text{-}22^{C22\text{-}OG488}$) was first mixed with saturating amounts of Sly1 (~300 nM). Then, an excess of the unlabeled N-peptide (1-21, ≈ 5 μM) was added and the dissociation of the N-peptide/Sly1 complex was monitored (orange curve). When the experiment was carried out in the presence of 15 μM of the remaining portion of the cytosolic domain of Sed5 (21-324), no significant change in the off-rate of the N-peptide/Sly1 complex was observed (blue curve), suggesting that the Sed5 21-324 does not influence the binding strength of the N-peptide. A similar result was obtained by titrations of Sly1 to Sed5 $1\text{-}22^{C22\text{-}OG488}$ in the absence or presence of Sed5 21-324 (data not shown).

Table S1: Thermodynamic parameters obtained by all ITC experiments in this study

Cell	Syringe	K_d (nM)	ΔH (kcal/ mole)	n
Sly1	Sed5 1-320	0.30 ± 0.11	-25.6 ± 0.16	1.01
Sly1	Sed5 1-210	0.24 ± 0.35	-18 ± 0.16	1.00
Sly1	Sed5 1-21	1.47 ± 0.45	-16 ± 0.13	0.98
Sly1	Sed5 21-324	-	-	-
Sly1	Sed5 211-320	-	-	-
Sly1	Sed5 1-320^{F10A}	234 ± 72	-8.98 ± 0.63	1.09
Sly1	Sed5 1-21^{F10A}	-	-	-
Sly1	Sed5 1-320^{I290A}	0.93 ± 0.24	-21.1 ± 0.12	1.04
Sly1	Sed5 1-210/ 211-320 complex	0.48 ± 0.49	-22.7 ± 0.20	0.92
Sly1	Quaternary SNARE complex containing Sed5 1-320	0.23 ± 0.30	-20.3 ± 0.22	0.88
Sly1	Quaternary SNARE complex containing Sed5 211-320	-	-	-
Sly1	Ufe1 1-21	34.4 ± 5.2	-15.8 ± 0.23	1.02
Sly1/Ufe1 1-21	Sed5 1-320	0.17 ± 0.09	-21.9 ± 0.37	0.85
Sly1/Ufe1 1-21	Sed5 1-210	-	-	-
Sed5 211-320	Sed5 1-210	2700 ± 400	+6.13 ± 0.34	0.98

All isothermal calorimetric experiments were performed at 25 °C in PBS buffer. The errors reported are the numbers obtained from fitting the data of a single ITC run. The experimental ITC data for each of the interactions are shown in Fig. S4.

References

1. Kloepper TH, Kienle CN, & Fasshauer D (2007) An elaborate classification of SNARE proteins sheds light on the conservation of the eukaryotic endomembrane system. *Mol Biol Cell* 18:3463-3471.
2. Flanagan JJ & Barlowe C (2006) Cysteine-disulfide cross-linking to monitor SNARE complex assembly during endoplasmic reticulum-Golgi transport. *J Biol Chem* 281:2281-2288.
3. Joglekar AP, Xu D, Rigotti DJ, Fairman R, & Hay JC (2003) The SNARE motif contributes to rbet1 intracellular targeting and dynamics independently of SNARE interactions. *J Biol Chem* 278:14121-14133.
4. Tsui MM, Tai WC, & Banfield DK (2001) Selective formation of Sed5p-containing SNARE complexes is mediated by combinatorial binding interactions. *Mol Biol Cell* 12:521-538.
5. Xu D, Joglekar AP, Williams AL, & Hay JC (2000) Subunit structure of a mammalian ER/Golgi SNARE complex. *J Biol Chem* 275:39631-39639.
6. Fasshauer D & Margittai M (2004) A Transient N-terminal Interaction of SNAP-25 and Syntaxin Nucleates SNARE Assembly. *J. Biol. Chem.* 279:7613-7621.
7. Yamaguchi T*, et al.* (2002) Sly1 binds to Golgi and ER syntaxins via a conserved N-terminal peptide motif. *Dev Cell* 2:295-305.
8. Dulubova I*, et al.* (2003) Convergence and divergence in the mechanism of SNARE binding by Sec1/Munc18-like proteins. *Proc Natl Acad Sci U S A* 100:32-37.
9. Braun S & Jentsch S (2007) SM-protein-controlled ER-associated degradation discriminates between different SNAREs. *EMBO Rep* 8:1176-1182.
10. Velazquez-Campoy A & Freire E (2006) Isothermal titration calorimetry to determine association constants for high-affinity ligands. *Nat Protoc* 1:186-191.

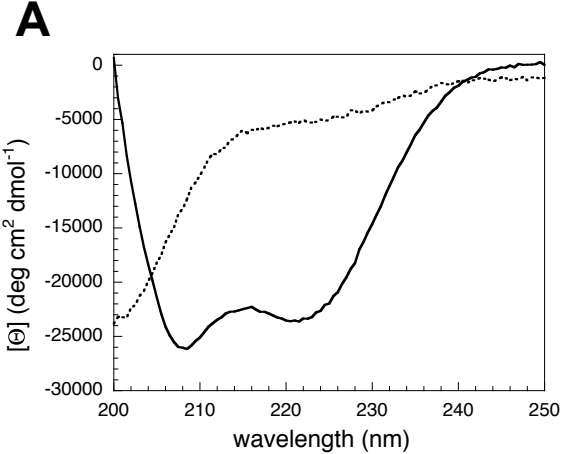
A
0
-5000
-10000
-15000
-20000
-25000
-30000
[Θ] (deg cm2 dmol-1)
200
210
220
230
240
250
wavelength (nm)

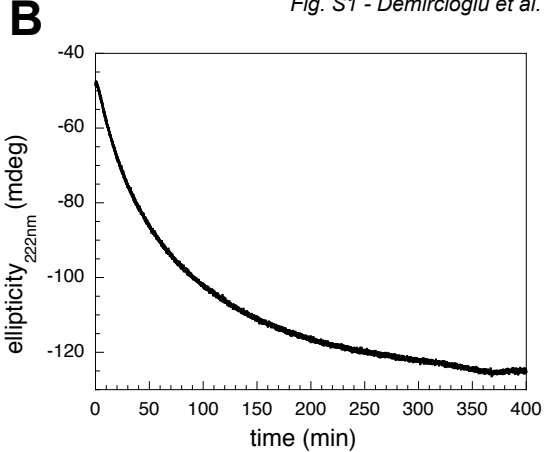
B
-40
-60
-80
-100
-120
ellipticity222nm (mdeg)
0
50
100
150
200
250
300
350
400
time (min)

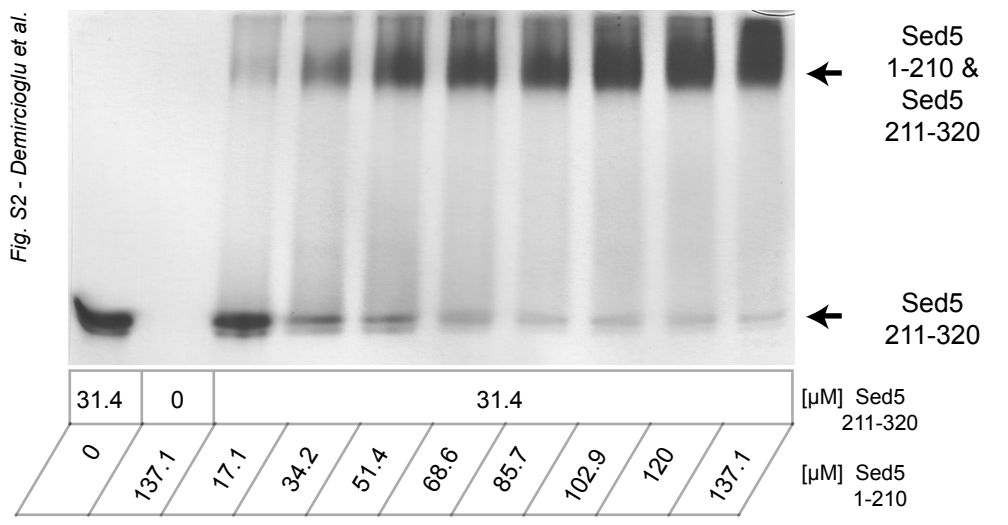
Fig. S2 - Demircioglu et al.
Sed5
1-210 &
Sed5
211-320
Sed5
211-320
31.4
0
31.4
[µM] Sed5
211-320
0
137.1
17.1
34.2
51.4
68.6
85.7
102.9
120
137.1
[µM] Sed5
1-210

Fig. S3 - Demircioglu et al.

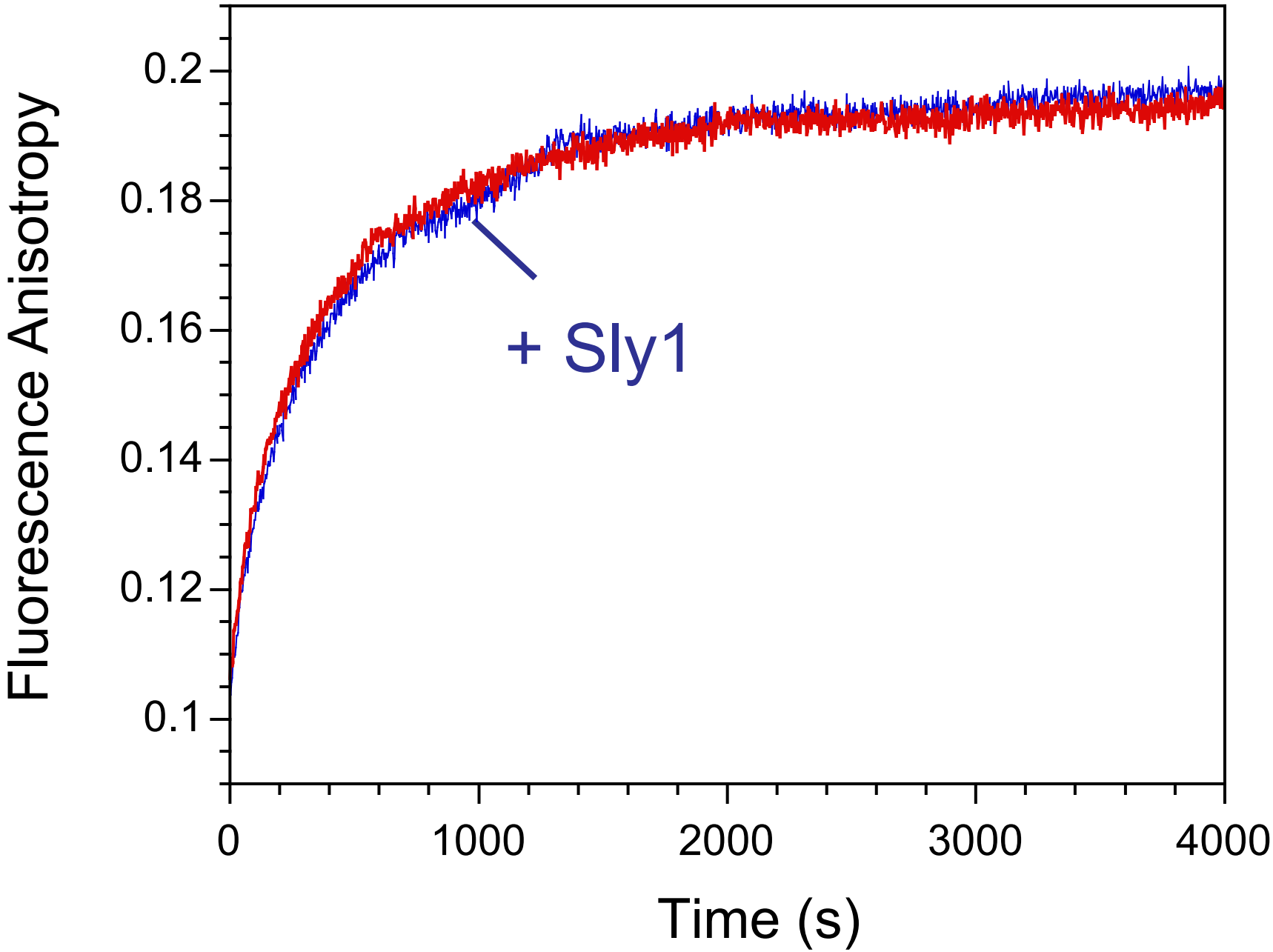

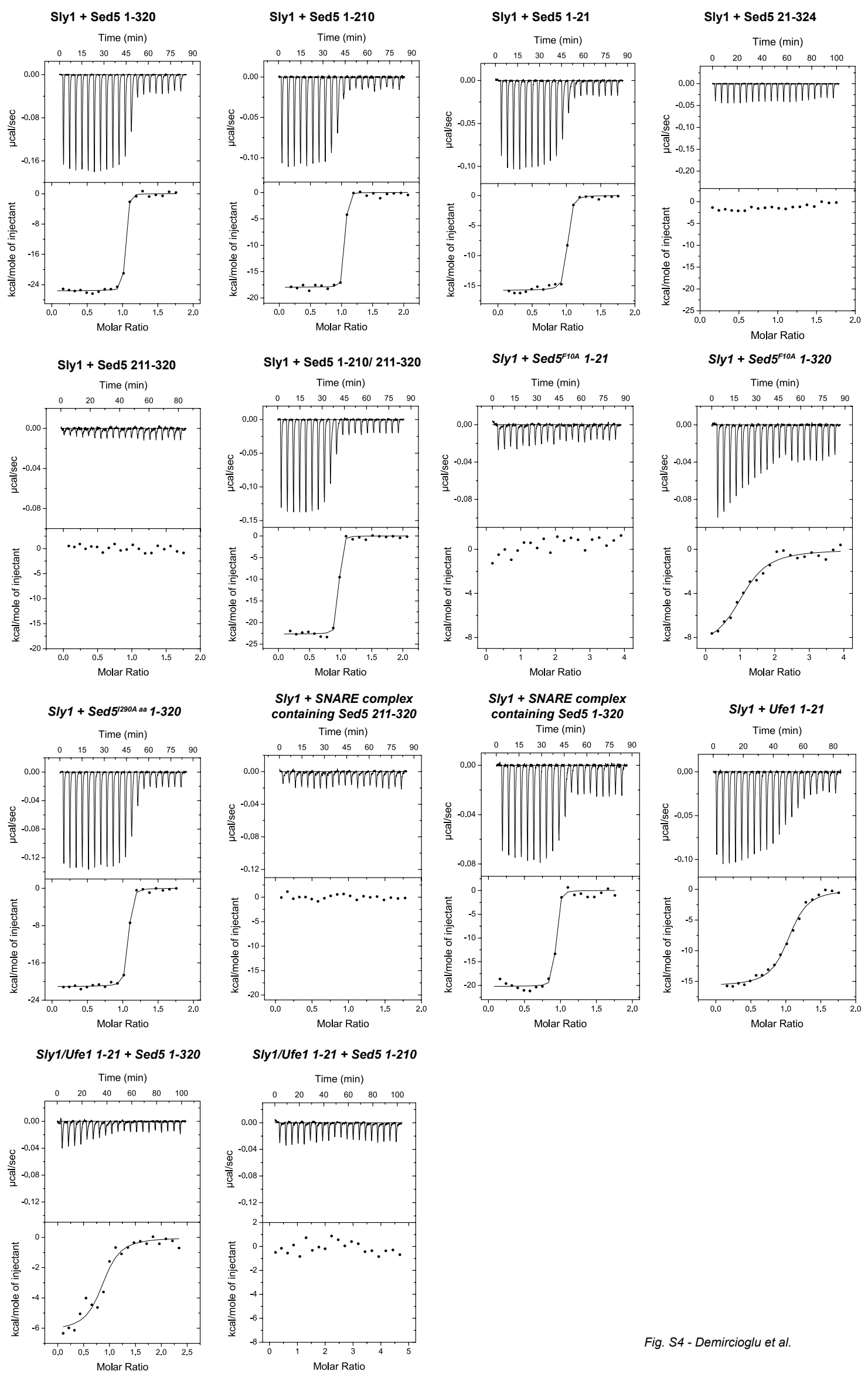

Fig. S4 - Demircioglu et al.

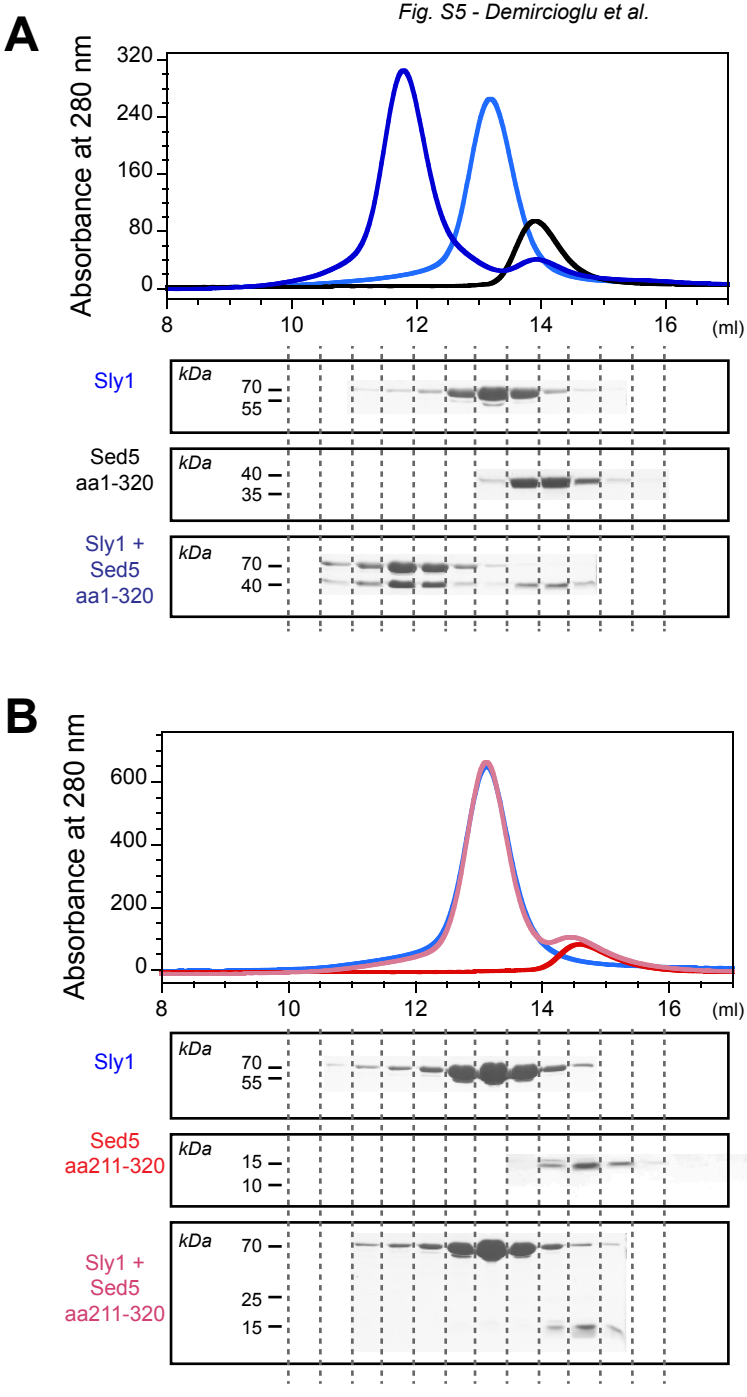
A
Absorbance at 280 nm
320
240
160
80
0
8
10
12
14
16
(ml)
Sly1
kDa
70
55
Sed5
aa1-320
kDa
40
35
Sly1 +
Sed5
aa1-320
kDa
70
40
B
Absorbance at 280 nm
600
400
200
0
8
10
12
14
16
(ml)
Sly1
kDa
70
55
Sed5
aa211-320
kDa
15
10
Sly1 +
Sed5
aa211-320
kDa
70
25
15

Fig. S6 - Demircioglu et al.